Journal of Applied Fluid Mechanics, Vol. 12, No. 3, pp. 883-890, 2019.
Available online at www.jafmonline.net, ISSN 1735-3572, EISSN 1735-3645.
DOI: 10.29252/jafm.12.03.29058

Numerical Investigation of Combustion Wave Propagation in Obstructed Channel of Pulse Detonation Engine using Kerosene and Butane Fuels

N. Alam†, K. M. Pandey and K. K. Sharma

Department of Mechanical Engineering, National Institute of Technology Silchar, Assam-788010, India

†*Corresponding Author Email: nooralam2011@gmail.com*

(Received April 2, 2018; accepted November 25, 2018)

ABSTRACT

The present computational analysis reports the results of combustion phenomenon in 1200 mm long and 60 mm internal circular diameter (D) of three dimensional obstructed combustion chamber (combustor) of the pulse detonation engine (PDE). The simulation is carried out for stoichiometric mixture of two fuels Kerosene-air and Butane-air mixture at atmospheric pressure and temperature of 1 atm and 300 K respectively along with preheated air. The chemical species of Kerosene and Butane ($C_{12}H_{26}$ and C_4H_{10}) fuel are solved by species transport equation and irreversible one-step chemical kinetics model. The propagation speed of flame, detonation wave pressure and deflagration-to-detonation transition (DDT) run-up length are analyzed by three dimensional reactive Navier–Stokes algorithm along with realizable k-ε turbulence equation model. The obstacles are placed inside the combustor tube at spacing (s) of 60 mm (1D) and obstacles having blockage ratio (BR) 0.5 for creating perturbation in propagating combustion flame. This resulted in increase of the surface area of propagating flame and reduces deflagration-to-detonation transition (DDT) run-up length.

Keywords: Obstacles; Turbulent flame; Detonation; PDE.

NOMENCLATURE

C-J	Chapman Jouguet
e	specific internal energy
h	specific enthalpy
k	turbulent kinetic energy
P	pressure
PDE	pulse detonation engine
q_j	heat flux
R_G	universal Gas Constant
W_i	molar weight
Y	fuel Mass Fraction
δ_{ij}	kronecker delta
ρ	density
τ_{ij}	viscous Stress Tensor
ε	turbulence dissipation rate

Subscripts

i	i^{th} component of species
j	j^{th} component of species

1. INTRODUCTION

The detonation wave in pulse detonation engine is extensively investigated experimentally, analytically and numerically since last 20th century (Gamezo and Oran 1997; Gamezo *et al.*, 1997; Denisov *et al.*, 1959; Voitsekhovsky *et al.*, 1963). So, it increases interest in present year due to their potential advantage in propulsion thrust over the conventional propulsion system. The PDE system has high specific impulse (I_{sp}) and thermodynamic efficiency compared to the other space-vehicles along with reduced complexity in mechanism of combustion (Mattisona *et al.*, 2005). The pulse detonation engine operates on the mechanism of supersonic combustion. The principle of PDE is that it operates on lower entropy production. However, the other propulsion system operates on deflagration mode at constant pressure process (Tangirala *et al.*, 2005). The circular cross-section of PDE tube gives better propulsive

performance over the rectangular cross-section tube (Jie *et al.,* 2014; Lu *et al.,* 2017; Kuznetsov *et al.,* 2002; Kellenberger and Ciccarelli, 2015; Zheng *et al.,* 2017). There are number of experimental and numerical models studied on the performance of PDE detonation tube at single cycle operation. (Nicholls *et al.,* 1957; Wintenberger and Shepherd, 2006) analyzed unsteady detonation wave generated and measured direct impulse. (Wood and Kirkwood, 1954) explained the ZND model refer to axial flow behind the spherical shock front. (Kapila and Roytburd, 1989) numerically simulated transition to detonation in 1-D by reactive Euler equations. It stated that explosive have low temperature non-uniformity in initial state and ZND (Zeldovich, yon Neumann, Döring) detonation created high temperature and high pressure by thermal explosion and supersonic reaction wave. (Majda and Roytbur, 1990) demonstrated computational analysis, the formation of exothermic reaction in the solutions of inviscid reactive mixture. (Taki and Fujiwara, 1978) numerically analyzed two-step reaction model of oxy-hydrogen mixture through 2-D unsteady hydrodynamic and chemical kinetic equations. Due to initial disturbances, they observed that the triple shock waves are generated and geometry of shock wave after the transition period for stoichiometric mixture ratio. The results show that the given geometry of detonation tube, any exothermic system has its own characteristic of multi-dimensional structure. (Zhang *et al.,* 2015) analyzed through chemical kinetic model to the direct detonation initiation by focusing shock waves when acetylene-air mixture entering axially and circumferentially at inlet in pulse detonation engine. The results show in static flow region, the detonation wave is produced when mixture entering circumferentially at Mach 2.4 and high pressure and temperature are created by shock focusing in the PDE combustor. However, in dynamic flow field increases Mach number for generating detonation wave. (Srihari *et al.,* 2015) studied simulations of compressible, transient and intermittent phenomenon by using one-step irreversible chemical reaction model in 1-D and 2-D axis symmetric tubes for reducing computational complexity. It shows that the phenomenon of fluid inside the detonation tube is the function of distance and time. They are also analyzed the Von-Neumann spike, detonation velocity and C-J Pressure with different grid size and found that one-step overall reaction model is predicted the flow properties with maximum accuracy. (Lu *et al.,* 2017) investigated through one-dimensional simulation of interaction between pressure wave and flame front by using Arrhenius expression with chemical model of hydrogen oxidation. They are observed the propagation and reflection of pressure wave might trigger in cylinder, and lead to very high-pressure oscillation. Chemical kinetics are analyzed intermediate radicals under higher pressure during auto-ignition. The gradient of ignition is used detonation initialization.

(Ma *et al.,* 2002) analyzed temperature and concentration of C_2H_4 through a newly developed diode-laser absorption sensor in the combustion process of PDE tube. Ignition timing and active control valve is successfully operated in the Stanford PDE tube for the optimization of fuel injection and achieving the impulse for each cycle constantly. Shimo *et al.* (2002) developed a PDE model by using ignition system and automobile valve. It is successfully operated by propane and ethylene gaseous fuels at different initialization conditions. Therefore, shock velocity is considered approximately equal to the C-J detonation velocity. (Driscoll *et al.,* 2016; 2015; 2015; 2013; 2012) investigated the initiation through DDT is vary with the system parameters such as operating frequency (f), fill fraction (ff_{Driver}), driver PDE length (L_{PDE}) driven PDE nitrogen dilution (n), start-up skin temperature (T_{Start}), and diameter (D_{Tube}). The fill fraction of driver PDE tube has largest effect on the ignition initiation within the driven PDE. The auto-ignition is reduced as reducing of the driver PDE length, due to increase of skin temperature of hot products from the driven PDE tube. Therefore, DDT run-up length is increased about 70% for initiation at room temperature (T_{Start}=297K). (Gaathaug *et al.,* 2012) investigated 2-D simulation of deflagration-to-detonation transition (DDT) of hydrogen-air mixtures in 3 m long square channel, which have one end closed with single obstacle placed 1 m from the end, and the other end opened in the atmosphere. The mixture is ignited at the closed end and DDT produced within 1 m behind the obstacle. (Kailasnath *et al.,* 1999; Ma *et al.,* 2002; Kailasanath and Patnaik, 2000) discussed that the outflow boundary condition was specified for flow field as well as estimation of overall performance. This study is not recommended with ideal boundary conditions. But also compared numerical simulations results with experimental data for taking correct boundary conditions.

The objective of the present study is to investigate the thermal property of combustion of two different fuel kerosene-air and butane-air mixture at ambient inlet condition. The cyclic processes of combustion are compared shock pressure and high speed detonation waves generated in the PDE combustion chamber by these fuels. The temperature of combustion flame is also analyzed and compared.

2. NUMERICAL METHODOLOGY

The combustion process in pulse detonation engine combustor is analyzed by solving three-dimensional Reynolds-averaged Navier-Stokes (RANS) equations, and two realizable k-ε turbulence equations with one-step irreversible chemical reaction model (Chapman and Cowling 1970; Smirnov *et al.,* 2017; Gnani *et al.,* 2018; Alam *et al.,* 2018). The computational analysis is considered compressible turbulence model and it is solved by species transport model along with eddy dissipation as well as finite rate chemistry model. The governing equations used in this analysis are described below.

2.1 Governing Equations

For the computing of combustion phenomena in three-dimensional PDE combustor, the governing equations are required to solved with state equations for independent variables.

Continuity equation

$$\frac{\partial \rho}{\partial t}+\frac{\partial}{\partial x_i}(\rho u_i)=0 \tag{1}$$

Momentum equation

$$\frac{\partial}{\partial t}(\rho u_i)+\frac{\partial}{\partial x_i}(\rho u_i u_j)=-\frac{\partial P}{\partial x_i}+\frac{\partial \tau_{ij}}{\partial x_i} \tag{2}$$

where τ_{ij} is the viscous stress tensor

$$\tau_{ij}=\mu\left(\frac{\partial u_i}{\partial x_j}+\frac{\partial u_j}{\partial x_i}-\frac{2}{3}\delta_{ij}\frac{\partial u_i}{\partial x_i}\right) \tag{3}$$

Energy equation

$$\frac{\partial}{\partial t}\left[\rho\left(e+\frac{1}{2}u_i u_i\right)\right]+\frac{\partial}{\partial x_j}\left[\rho u_i\left(h+\frac{1}{2}u_i u_i\right)\right]= \frac{\partial}{\partial x_j}\left(u_i \tau_{ij}\right)-\frac{\partial q_j}{\partial x_j} \tag{4}$$

where x_j and u_j are the j^{th} component of position vector velocity

and $h=e+P/\rho$ (5)

where, the algebraic relation of equation of state is

$$\rho=\sum_{i=1}^{n}Y_i\rho_i,\ P=R_G T\sum_{i=1}^{n}\frac{\rho_i}{W_i} \tag{6}$$

where, $i=n^{th}$ species

and $Y_n=\sum_{i=1}^{n-1}Y_i$ (7)

2.2 Species Transport Equation

$$\frac{\partial c}{\partial t}+\frac{\partial}{\partial x_i}(u_i c)=\frac{\partial}{\partial x_i}\left(D_{ij}\frac{\partial c}{\partial x_i}\right)+S \tag{8}$$

here, C is the concentration of chemical species, u_i is velocity, D_{ij} is diffusion coefficient and S is source term, and the Diffusion coefficient is solved by using the Chapman and Cowling equation (Dzieminska and Hayashi, 2013)

$$D_{ij}=1.8829\times10^{-2}\frac{\sqrt{T^3 m_{ij}}}{p\sigma_{ij}^2\Omega_D} \tag{9}$$

where, mole mass m, collision diameter σ and collision diffusion integer Ω_D are calculated by the equations given below

$$m_{ij}=\frac{m_i m_j}{m_i+m_j} \tag{10}$$

$$\sigma_{ij}=\frac{1}{2}(\sigma_i+\sigma_j) \tag{11}$$

$$\Omega_D=\left(\frac{T}{T_{\varepsilon ij}}\right)^{-0.145}+\left(\frac{T}{T_{\varepsilon ij}+0.5}\right)^{-2} \tag{12}$$

The binary diffusion coefficient D_i is

$$D_i=\frac{1-Y_i}{\sum_{j\neq i}X_j/W_j} \tag{13}$$

and $X_i=\frac{Y_i/W_i}{\sum_{j=1}^{n}Y_j/W_j}$ (14)

The viscosity coefficients for the gaseous mixture are (Bird *et al.*, 1960)

$$\mu_i=2.6693\times10^{-5}\frac{\sqrt{W_i T}}{\sigma_i^2\Omega_\upsilon} \tag{15}$$

where W_i is the molecular weight of i^{th} species, σ_i is collisions diameter in Angstrom unit, and Ω_υ expresses collision integrals expressed by

$$\Omega_\upsilon=1.147\left(\frac{T}{T_{ei}}\right)^{-0.145}+\left(\frac{T}{T_{ei}+0.5}\right)^{-20} \tag{16}$$

where T_{ei} is effective temperature of species

2.3 Turbulence Model

The realizable k-ε turbulence model based on transport equations of turbulent kinetic energy (k) and dissipation rate (ε):

$$\frac{\partial}{\partial t}(\rho k)+\frac{\partial}{\partial x_j}(\rho k u_j)=\frac{\partial}{\partial x_j}\left[\left(\mu+\frac{\mu_t}{\sigma_k}\right)\frac{\partial k}{\partial x_j}\right]+ P_k+P_b-\rho\varepsilon-Y_M+S_k \tag{17}$$

and

$$\frac{\partial}{\partial t}(\rho\varepsilon)+\frac{\partial}{\partial x_j}(\rho\varepsilon u_j)=\frac{\partial}{\partial x_j}\left[\left(\mu+\frac{\mu_t}{\sigma_\varepsilon}\right)\frac{\partial \varepsilon}{\partial x_j}\right]+ \rho C_1 S\varepsilon-\rho C_2\frac{\varepsilon^2}{k+\sqrt{\nu\varepsilon}}+C_{1\varepsilon}\frac{\varepsilon}{k}C_{3\varepsilon}P_b+S_\varepsilon \tag{18}$$

where,

$$C_1=\max\left[0.43,\frac{\eta}{\eta+5}\right] \tag{19}$$

$$\eta=S\frac{k}{\varepsilon},\ S=\sqrt{2S_{ij}}S_{ij} \tag{20}$$

where, P_k and P_b represent the generation of turbulence kinetic energy due to the mean velocity gradient and due to buoyancy respectively, and σ_κ and σ_ε are the turbulent Prandtl numbers for *k* and ε.

2.4 Computational Domain

The geometry of three-dimensional computational model is considered as a cylindrical obstructed PDE tube having 60 mm inner circular diameter and 1200 mm long straight tube as shown in Fig. 1. The computational combustion model contained obstacles of blockage ratio (BR) 0.5 with 60 mm spacing (s) among them for obtaining better

combustion mechanism. The blockage ratio of the obstacle is calculated by Eq. (21).

$$BR = \left(1 - \frac{{d_{obs}}^2}{{D_{obs}}^2}\right) \tag{21}$$

where,

d_{obs} = inner diameter of obstacle

D_{obs} = outer diameter of obstacle

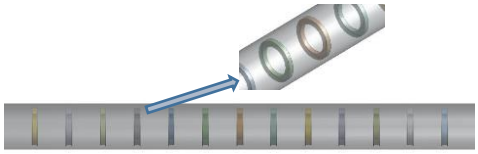

Fig. 1. 3-D Computational model of PDE tube obstacles of BR=0.5 and spacing S=1D.

2.5 Grid Convergence Criteria

For simulation purpose, the grid is automatic generated on the entire domain of PDE combustor as shown in Fig. 2. The tetra and hexahedral dominant mesh are generated with 4.1 mm element size by using ANSYS ICEM CFD. The meshing of computational domain has high impact on the simulation results. Therefore, for obtaining better results with some constraints such as simulation time and computational cost, etc. The mesh is refined as shown in Fig. 3. The grid independence test is done for obtaining an optimum element size at which it gives maximum accuracy in the results without farther refinement of mesh. The refinement element is given in Table 1. The orthogonal quality and minimum error is considered about 0.998 and 0.001 %, respectively for the above (4.1 mm) elements size.

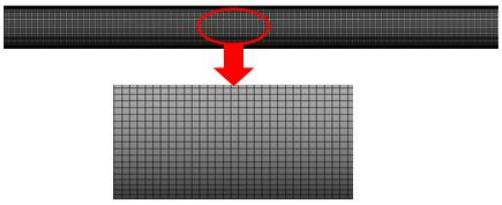

Fig. 2. Mesh generated on three-dimensional PDE Tube of BR-0.5.

2.6 Initial and Boundary Conditions

There are mainly three types of boundary conditions inflow, out flow, and fixed wall applied on the combustion model. The initial boundary conditions are applied to the fuel and air at inlet (inflow) for initiation of combustion as shown in Table 2. The right side of the combustion chamber is considered as an open end and fixed pressure outlet boundary condition. The cylindrical wall is assigned as insulated surface as well as no slip condition. Therefore, normal velocity, temperature gradient, and mass flux at adiabatic wall should be zero (Eq. 22).

$$u.n = 0,\ \frac{\partial T}{\partial x} = 0,\ \frac{\partial Y_k}{\partial x} = 0 \tag{22}$$

For the numerical analysis of two different fuels, the stoichiometric ratio (ϕ=1) of fuel-air mixture is calculated by Eqs. (23)-(25). The fuel butane-air and kerosene-air (C_4H_{10}-air & $C_{12}H_{26}$-air) are taken as ideal gas. The impermeability condition for closed model is expressed by Eq. (26) (Gnani *et al.*, 2018):

$$C_mH_n + \left(m + \frac{n}{4}\right)(O_2 + 3.76N_2) \rightarrow mCO_2 + \frac{n}{2}H_2O + \left(m + \frac{n}{4}\right) \times 3.76N_2 \tag{23}$$

$$\phi = \frac{F/A}{(F/A)_{st}} \tag{24}$$

$$\text{where } (F/A)_{st} = \frac{1}{4.76(m + n/4)}\frac{W_f}{W_a} \tag{25}$$

where W_f is a molecular weight of fuel and W_a is a molecular weight of air.

$$u.n = 0 \text{ given } x \in \partial\Omega \tag{26}$$

where $\partial\Omega$ is boundary of working region, n is normal vector at that point. For numerical analysis the Eq. (16) and Eq. (2) are co-related and given that the normal pressure derivative to the wall is zero.

$$n.\Delta p = 0 \text{ given } x \in \partial\Omega \tag{27}$$

Table 1 Mesh refinement level for PDE tube.

S. No.	Number of elements	Flame velocity (m/s)	Error (%)
1	3,50,043	1739.53	-
2	3,84,948	1743.03	0.200
3	3,98,946	1744.11	0.062
4	**4,18,016**	**1744.45**	0.019
5	4,55,380	1744.45	**0.001**

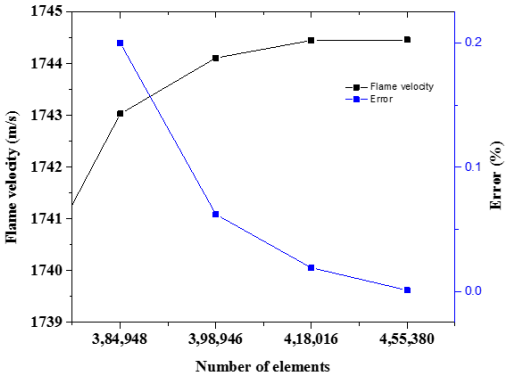

Fig. 3. Grid convergence analysis of PDE tube.

Table 2 Input parameters of stoichiometric fuel-air mixture for PDE.

Inlet parameter	Air	Hydro-fuel
Pressure (atm)	1	1
Temperature (K)	950	300
Mass flow rate of $C_{12}H_{26}$ (Kg/s)	0.655	0.04392
Mass flow rate of C_4H_{10} (Kg/s)	0.655	0.04265
O_2 mass fraction	0.23	0
Hydro-fuel mass fraction	0	1
H_2O mass fraction	0.032	0

2.7 Combustion Modeling

Semi-Implicit Method for Pressure Linked Equations-Consistent (SIMPLEC) algorithm is used for solving three-dimensional Navier-Stokes equations along with one-step chemical kinetics model. The species transport equation is used to combustion of stoichiometric fuel mixture by using eddy dissipation as well as finite rate chemistry model.

Assumptions:

- The combustion analysis is considered as a steady state flow condition.
- The fuel gases are assumed to be follow ideal gas law and having compressibility effect.
- The turbulence model is used realizable two equation $k-\varepsilon$ model.
- The 3D N-S equation are solved with second order accuracy.

3. Results And Discussions

The present computational analysis on the basis of flame propagation velocity and detonation pressure (generated inside the combustor) are validated with the experimental results obtained by (Kuznetsov *et al.*, 2002) at atmospheric boundary conditions of pressure and temperature. They analyzed the flame velocity of 10 % CH_4 –air mixture at atmospheric initial conditions of temperature and pressure 293 K and 1 atm respectively in the obstructed PDE tube. The propagating flame has been attained a steady-state speed about 1750 m/s, below the theoretical Chapman-Jouguet (C-J) detonation velocity and the detonation pressure is about 20.7 atm. (Card *et al.*, 2005) also experimentally investigated the flame velocity for different fuels such as: ethylene, hydrogen, JP-10 and acetylene. They observed that the flame velocity quickly increases from isobaric speed of sound to the Chapman–Jouget detonation velocity of 1848 m/s. The combustion mechanism of gasoline-air mixture is analyzed by (Gordon and McBride 1994) through NASA CEA400 code and calculated the flame velocity of about 1796 m/s and pressure is 18.85 atm at same atmospheric initial pressure and temperature. The predicted value of detonation velocity and pressure of shock wave for different researcher are shown in Table 3. The present computational model is verified with the experimental results of (Card et al.., 2005) by taking same acetylene-air mixture and obstructed combustion chamber. The velocity and pressure are approximately similar to the experimental results of (Card et al.., 2005) and others as shown in Table 3.

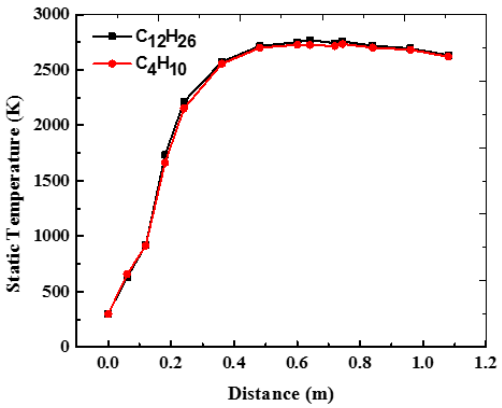

Fig. 4. Flame temperature of kerosene and butane fuels in PDE tube.

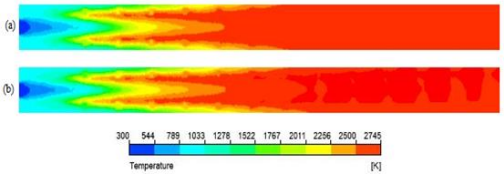

Fig. 5. Contours of run-up length of high temperature propagating flame for (a) kerosene and (b) butane fuels in the PDE tube.

The combustion of kerosene-air and butane-air mixture are computationally analyzed in the obstructed combustion chamber of pule detonation engine. The exothermic reaction between fuel and air is initialized with one-step chemical kinetic model in the combustion chamber. The combustion is started in thermal explosion form and produced high temperature and high pressure detonation wave, and propagated towards the open end of the combustor tube. The reflected waves are propagated in opposite direction (towards the ignition zone). At inlet regime the static pressure of detonation wave is high. However, the dynamic pressure of detonation wave is high at outlet regime. The comparison of static flame temperature for both fuels in combustion chamber are shown in Fig. 4 and flame propagation run-up length is shown in Fig. 5.

The flame temperature of kerosene-air mixture is comparatively greater than the flame temperature of butane-air mixture. Therefore, high temperature fully developed combustion takes place early as possible in the entire zone of combustor. The obstacles are fixed inside the tube at equal distance of 60 mm to each other, which is caused perturbation in the flame propagation medium and generated strong Mach stems. This turbulent flame trying to complete burning of all fuel particles as early as possible and reduces the flame run-up distance.

Table 3 Validation of the present computation model with experimental studies.

S. No.	Author	Detonation Pressure (atm)	Detonation Velocity (m/s)	Fuel
1	Kuznetsov *et al.* (2002)	20.7	1750	Methane
2	Card *et al.*, 2005	-	1848	Ethylene, Hydrogen, JP-10 and Acetylene
3	Gordon and McBride, 1994	18.85	1796	Gasoline
4	Present model	17.68	1778	Ethylene

The obstacles are created perturbation in combustion flow regime, which increases the momentum of burnt fuel particles and turbulence in propagating medium. Therefore, leading flame edge is tried to burn all neighboring fuel particle and produced high temperature combustion regime in which flame accelerates with high speed. The obstacles blockage ratio is also limited for increase of flame velocity. As the blockage ratio of obstacles is increased (the propagating medium or flow normal area reduces) the speed of combustion products is increased. The velocity of kerosene air mixture and butane air mixture is as shown in Fig. 6. Initially combustion is started in the deflagration mode and then flame propagated below the speed of sound (about 300 m/s) up to 250 mm from inlet wall. After that flame attain detonation speed at the end of combustor. The velocity of butane-air and kerosene-air mixture have very small difference between them. The combustion flame velocity for butane-air mixture is comparatively higher than the kerosene-air mixture in the imitation of combustion. Because of, butane fuel is vaporized easily due to gaseous phase and kerosene fuel is not vaporized easily due to liquid form.

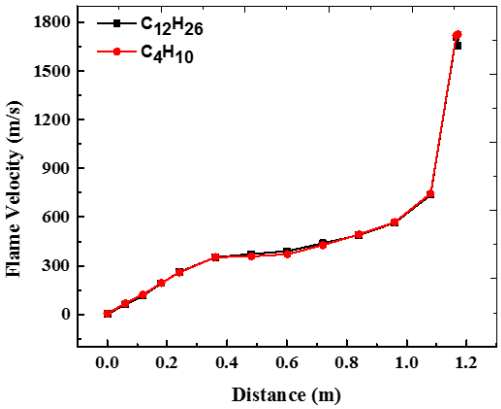

Fig. 6. Flame velocity of kerosene and butane fuels in PDE tube.

The pressure of shock wave is as shown in Fig. 7. The static pressure of butane-air is comparatively 0.58 % higher than the static pressure of kerosene-air mixture and reached its peak value in initial stage and then decreased towards the open end of combustor. The leading edge of combustion flame is compressed by hot gas towards the open end. Therefore, reflected wave are travelled towards the inlet zone. This high temperature reflected shock wave are pre-heat to the incoming fresh fuel-air mixture for the continuous generation and the propagation of high temperature and high pressure combustion wave. The reflected shock wave is also generated a hot spot near the wake of obstacles. Therefore, detonation wave is deflagrated from high pressure zone to the low pressure zone very high speed (above the sound speed).

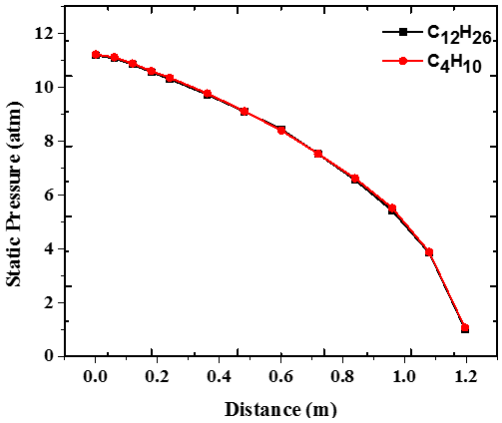

Fig. 7. Shock pressure of kerosene and butane fuels in PDE tube.

5. CONCLUSIONS

The combustion analysis of kerosene-air and butane-air mixture has been done by species transport combustion model. The combustion wave is propagated in obstacle laden combustor of pulse detonation engine. The obstacles are used to create turbulence in combustion regime. So that, it increases the flame surface area, which caused to complete burning of inlet fuel-air mixture particles.

- The simulation results show that the butane-air mixture is better than the kerosene-air mixture.

- A high temperature and pressure shock wave are generated in combustion chamber. The peak pressure of detonation waves for butane-air mixture is about 0.58 % higher than the static pressure of kerosene-air mixture.
- The combustion flame velocity of butane-air mixture is comparatively higher than the flame velocity of kerosene-air mixture. which is lower than the C-J detonation velocity (Gordon and McBride, 1994).
- The high temperature flame is propagated and collided with the obstacles, which caused to reduce the DDT run-up length and produce the fully developed combustion zone early as possible. The DDT run-up length for both fuel is obtained approximately similar.

REFERENCES

Alam, N., K. K. Sharma and K. M. Pandey (2018). Numerical investigation of combustion phenomena in pulse detonation engine with different fuels, *AIP Conference, Proceedings* 1966, 020015 (2018).

Bird, R. B., W. E. Stewart and Lightfoot EN (1960). *Transport phenomena*, Wiley.

Chapman, S. and T. G. Cowling (1970). *The mathematical theory of non-uniform gases*. Cambridge University Press.

Denisov, Y. N., Y. K. Troshin and D. A. Nauk SSSR (1959). *Phys-Chem. Sec.*, 125, 110-113.

Driscoll, R., A. St. George, D. Munday and E. J. Gutmark (2016). Optimization of a multiple pulse detonation engine-crossover system. *Applied Thermal Engineering* 96, 463-472.

Driscoll, R., A. St. George, D. Munday and E. J. Gutmark (2013). Experimental Study of Sustained Shock Initiated Detonation in a Multiple Pulse Detonation-Crossover System. *51st AIAA Aerospace Sciences Meeting including the New Horizons Forum and Aerospace Exposition*, 7-10 January.

Driscoll, R., W. Stoddard, A. St. George and E. Gutmark (2015). Shock Transfer and Shock-Initiated Detonation in a Dual Pulse Detonation Engine/Crossover System, *AIAA JOURNAL*, 53(1).

Driscoll, R., A. St. George, W. Stoddard, D. Munday, and E. J. Gutmark (2015). Characterization of Shock Wave Transfer in a Pulse Detonation Engine-Crossover System, *AIAA Journal* 53(12).

Driscoll, R., W. Stoddard, Andrew St. George, B. Romanchuk, D. Munday and E. J. Gutmark (2012). Parametric Study of Direct Detonation Initiationfrom Shock Transfer through a Crossover Tube. *50th AIAA Aerospace Sciences Meeting including the New Horizons Forum and Aerospace Exposition*, 9-12 January.

Dzieminska, E. and A. K. Hayashi (2013). Auto-ignition and DDT driven by shock wave e Boundary layer interaction in oxyhydrogen mixture. *International Journal of hydrogen Energy* 38, 4185-4193.

Gaathaug, A. V., K. Vaagsaether, D. Bjerketvedt (2012). Experimental and numerical investigation of DDT in Hydrogen-Air behind a single obstacle. *International Journal of Hydrogen Energy* 37, 17606-17615.

Gamezo, V. N. and E. S. Oran (1997). Reaction-Zone Structure of a Steady-State Detonation Wave in a Cylindrical Charge. *Combustion and Flame* 109, 253-265.

Gamezo, V. N., D. Desbordes and E. S. Oran (1999). Formation and Evolution of Two-dimensional Cellular Detonations. *Combustion and Flame* 116, 154-165.

Gnani, F., H. Zare-Behtash, C. White and K. Kontis (2018). Effect of back-pressure forcing on shock train structures in rectangular channels. *Acta Astronautica*. 145, 471-481.

Gordon, S. and B. J. McBride (1994). *Computer program for calculation of complex chemical equilibrium compositions and applications (I): analysis*, Washington, D.C., NASA, Oct. Report No.: NASA RP-1311

Jie, L., Z. Longxi, W. Zhiwu, P. Changxin and C. Xinggu (2014). Thrust measurement method verification and analytical studies on a liquid-fueled pulse detonation engine. *Chinese Journal of Aeronautics* 27(3), 497-504.

Kailasanath, K. and G. Patnaik (2000). Performance Estimates of Pulsed Detonation Engines. *Proceedings of the Combustion Institute* 28, 595-601.

Kailasanath, K., and G. Patnaik (2000). Performance Estimates of Pulsed Detonation Engines, *Proceedings of the Combustion Institute* 28, 595-601.

Kailasanath, K., G. Patnaik and C. Li (1999). Computational Studies of Pulse Detonation Engines: A Status Report," *35th AIAA/ASME/SAE/ASEE* Joint Propulsion Conference and Exhibit, 20-24 June.

Kellenberger, M. and G. Ciccarelli (2015). Propagation mechanisms of supersonic combustion waves. *Proceedings of the Combustion Institute* 35, 2109-2116.

Kuznetsov, M., G. Ciccarelli, S. Dorofeev, V. Alekseev, Yu. Yankin and T. H. Kim (2002). DDT in methane-air mixtures. *Shock Waves* 12, 215-220.

Lu, W., W. Fan, K. Wang, Q. Zhang and Y. Chi (2017). Operation of a liquid-fueled and valveless pulse detonation rocket engine at high frequency. *Proceedings of the Combustion Institute* 36, 2657-2664.

Ma, L., S. T. Sanders, J. B. Jeffries and R. K.

Hanson (2002). Monitoring and Control of a Pulse Detonation Engine Using a Diode-Laser Fuel Concentration and Temperature Sensor. *Proceedings of the Combustion Institute* 29, 161–166.

Majda, A. J. and V. Roytbur (1990). Numerical Study of the Mechanisms for Initiation of Reacting Shock Waves, *SIAM Journal on Scientific and Statistical Computing* 11(5), 950-974.

Mattisona, D. W., M. A. Oehlschlaeger, C. I. Morris, Z. C. Owens, E. A. Barbour, J. B. Jeffries and R. K. Hanson (2005). Evaluation of pulse detonation engine modeling using laser-based temperature and OH concentration measurements. *Proceedings of the Combustion Institute* 30, 2799-2807.

Nicholls, J. A., H. R. Wilkinson and R. B Morrison (1957). Intermittent Detonation as a Thrust-Producing Mechanism. *Jet Propulsion* 27(5), 534-541.

Shimo, M., S. E. Meyer and S. D. Heister (2002). An Experimental and Computational Study of Pulsed Detonations in a Single Tube. *38th AIAA/ASME/SAE/ASEE Joint Propulsion Conference & Exhibit*, 7-10 July.

Smirnov, N. N., O. G. Penyazkov, K. L. Sevrouk, V. F. Nikitin, L. I. Stamov and V. V. Tyurenkova (2017). Detonation onset following shock wave focusing. *Acta Astronautica* 135, 114-130.

Srihari, P., M. A. Mallesh, G. Sai Krishna Prasad, B.V.N. Charyulu and D.N. Reddy (2015). Numerical Study of Pulse detonation engine with one-step overall reaction model. *Defence Science Journal* 65(4), 265-271.

Taki, S. and T. Fujiwara (1978). Numerical Analysis of Two-Dimensional Nonsteady Detonations. *AIAA Journal* 16(1).

Tangirala, V. E., A. J. Dean, P. F. Pinard and B. Varatharajan (2005). Investigations of cycle processes in a pulsed detonation engine operating on fuel–air mixtures. *Proceedings of the Combustion Institute* 30, 2817-2824.

Voitsekhovsky, B. V., V. V. Mitrofanov, and M. E. Topchian, (1969). Structure of a Detonation Front in Gases (Survey), *Combustion, Explosion, and Shock Waves* 5(3), 385-395.

Wintenberger, E. and J. E. Shepherd (2006). A model for the performance of air-breathing pulse detonation engines. *Journal of Propulsion and Power* 22(3), 593-603.

Wood, W. W. and J. G. Kirkwood (1954). Diameter effect in condensed explosive. The relation between velocity and rediuos of curvature of the detonation wave, *The Journal of Chemical Physics* 22(11), 1920-1924.

Zhang, Z., Z. Li and G. Dong (2015). Numerical Studies of Multi-Cycle Acetylene-air Detonation Induced by Shock Focusing. *Procedia Engineering* 99, 327-331.

Zheng, K., M. Yu, L. Zheng, X. Wen, T. Chu and L. Wang (2017). Experimental study on premixed flame propagation of hydrogen/methane/air deflagration in closed ducts, *International Journal of hydrogen energy* 42, 5426-5438.